Hindawi
Advances in Civil Engineering
Volume 2022, Article ID 5586737, 19 pages
https://doi.org/10.1155/2022/5586737

Research Article

Predicting Compressive Strength of Concrete Containing Industrial Waste Materials: Novel and Hybrid Machine Learning Model

Mohammed Majeed Hameed,[1] **Mustafa Abbas Abed**,[1] **Nadhir Al-Ansari**,[2] **and Mohamed Khalid Alomar**[1]

[1]*Department of Civil Engineering, Al-Maarif University College, Ramadi, Iraq*
[2]*Civil Engineering Department, Environmental and Natural Resources Engineering, Lulea University of Technology, Lulea 97187, Sweden*

Correspondence should be addressed to Mohammed Majeed Hameed; mohmmag1@gmail.com and Nadhir Al-Ansari; nadhir.alansari@ltu.se

Received 29 March 2021; Revised 11 February 2022; Accepted 5 March 2022; Published 23 March 2022

Academic Editor: Dawei Yin

In the construction and cement manufacturing sectors, the development of artificial intelligence models has received remarkable progress and attention. This paper investigates the capacity of hybrid models conducted for predicting the compressive strength (CS) of concrete where the cement was partially replaced with ground granulated blast-furnace slag (FS) and fly ash (FA) materials. Accurate estimation of CS can reduce the cost and laboratory tests. Since the traditional method of calculation CS is complicated and requires lots of effort, this article presents new predictive models called SVR – PSO and SVR – GA, that are a hybridization of support vector regression (SVR) with improved particle swarm algorithm (PSO) and genetic algorithm (GA). Furthermore, the hybrid models (i.e., SVR – PSO and SVR – GA) were used for the first time to predict CS of concrete where the cement component is partially replaced. The improved PSO and GA are given essential roles in tuning the hyperparameters of the SVR model, which have a significant influence on model accuracy. The suggested models are evaluated against extreme learning machine (ELM) via quantitative and visual evaluations. The models are evaluated using eight statistical parameters, and then the SVR-PSO has provided the highest accuracy than comparative models. For instance, the SVR – PSO during the testing phase provided fewer root mean square error (RMSE) with 1.386 MPa, a higher Nash–Sutcliffe model efficiency coefficient (NE) of 0.972, and lower uncertainty at 95% (U_{95}) with 28.776%. On the other hand, the SVR – GA and ELM models provide lower accuracy with RMSE of 2.826 MPa and 2.180, NE with 0.883 and 0.930, and U_{95} with 518.686 183.182, respectively. Sensitivity analysis is carried out to select the influential parameters that significantly affect CS. Overall, the proposed model showed a good prediction of CS of concrete where cement is partially replaced and outperformed 14 models developed in the previous studies.

1. Introduction

1.1. Background. As an essential in most civil engineering projects and activities, concrete is a standard man-made mixture consisting of specific components such as cement, water, and some additional materials. Since concrete manufacturing, many engineering projects have been carried out successfully using this profitable and imperative material. Traditional concrete is widely used in several construction areas, containing four classical materials: Portland cement, water, coarse aggregate, and fine aggregate. There is also a second type of concrete called high-strength concrete, which has unique properties due to the usage of additional materials that may not be used in ordinary concrete mixes. However, the estimation of hardened concrete properties is a critical obstacle for concrete technology due to several predicted and unpredicted parameters that may significantly influence the concrete properties [1, 2].

The compressive strength (CS) is one of the significant properties of concrete as it has a crucial role in designing engineering structures. Furthermore, other important properties of concrete, like water tightness and elastic modulus, have direct and significant relations with the CS of concrete. In current practice, to assess the CS of the concrete, many cylindrical or cubic samples are produced and tested at various sample ages. However, the conducted tests are time-consuming and expensive [3, 4]. Besides, the changes in the concrete mixes may lead to producing concrete with undesired characteristics. Hence, the tests should be repeated until the required properties of concrete are achieved by changing the magnitudes of the used ingredients [5]. Thus, this problem can be better encountered when pozzolan powders partially replace the cement content.

1.2. Using Ground Granulated Blast-Furnace Slag and Fly Ash Materials in the Concrete Mixture. As a type of pozzolan powders, ground granulated blast-furnace slag (FS) and fly ash (FA) are generally used as a partial replacement material of concrete because they are easy to reach and economic [6, 7]. In general, FA is a fine powder of spherical particles (diameter of 1 μm to 150 μm) obtained as a residual from the burning of pulverized coal in thermal power plant furnaces. As a result of its good performance and economic benefits, fly ash is used as a replacement for cement in 98% of American ready-mix companies [8]. As fly ash is an essential material in concrete mixture and thus it significantly affects the CS of concrete, several factors affect the characteristics of fly ash, such as the source of coal, heating and cooling mechanism, and combustion temperature [9]. The combustion process has a significant influence on the mechanical properties of FA. For instance, wet processing produces a FA with a high separated aggregate. On the other hand, dry processing can grow homogenous FA in particle size [10]. The utilization of FA material as partial replacement of cement in concrete mixture decreases the values of some concrete parameters like slump and CS. Still, it enhances the integrity and workability of the concrete [11]. Some studies recommend that in standard engineering and construction projects, the percentage of FA in concrete as a partial substitute for cement ranges from 20% to 50% of the total volume of cementitious aggregate [12]. However, concrete with fly ash increases the setting time; therefore, the CS of concrete varies by time and temperature of curing. Furthermore, fly ash concrete indicates an early development in concrete strength, particularly at elevated temperatures, which increases the CS in later stages compared to ordinary concrete [13].

Furnace slag (FS) is also considered a popular material used as partial cement replacement material. FS is a by-product of the manufacture of iron and steel in blast furnaces, the chemical composition of which is based on the raw materials from which it is produced [14]. Cooling status has great importance on the characteristics of the FS. For instance, if the molten slag is quickly cooled, it will be converted to noncrystalline components with hydraulic properties [15]. Additionally, concrete with higher CS and durability results in partial cement replacement with FS. However, a higher FS dosage can cause cracks and thermos-hygral (TH) damages, thereby negatively affecting the mechanical strength of concrete [16, 17].

The use of mentioned materials such as FS and fly ash in concrete as a partial replacement of cement is not only an effective waste disposal means but can be helpful as an alternative material for cement. Recent studies illustrated that the production of cement from different industries around the world case too much pressure on the environment by increasing the amount of carbon dioxide (CO_2) emissions in the atmosphere and, subsequently, global warming [18–20]. However, in the traditional concrete mixture, the relationship between the predictors (water, cement, fine and coarse aggregate) and CS property is nonlinear and challenging to capture. Furthermore, when the additives and other materials are used in concrete, such as FS and FA, CS and its parameters will become more complex. According to what mentioned before, there are no clear guidelines to select the optimum amount of FA and FS in concrete to ensure getting a desirable value of CS; therefore, a better understanding of that relation between CS and its variables using advanced approaches can help eliminate the carrying on the experiments and thus, reducing cost and time. Besides, it provides engineers with a simplified method to predict experimental outcomes.

Nevertheless, accurately predicting the CS of concrete where the cement martial is partially replaced has become a challenging issue in the concrete technology sector due to the complex and nonlinear relationship between CS property and the other materials used in manufacturing the concrete. Over the last decades, several scholars have developed models to estimate concrete CS. Moreover, scholars' attempts can be roughly divided into categories: (1) conventional artificial intelligence approaches such as soft computing models; (2) hybrid artificial intelligence models.

1.3. Soft Computing Models. Soft Computing (SC), as an efficient approach, can estimate the magnitude of the CS of concrete. One of the significant SC advantages is providing solutions for linear and nonlinear problems where the mathematical models cannot easily derive the under relation among the involved parameters in a particular situation [21]. Furthermore, SC methods utilize human-based knowledge, understanding, recognition, and learning in computing. Recently, many researchers have used artificial intelligence (AI) approaches and machine learning (ML) techniques as a sub-branch of SC methods to predict different concrete properties. Keshavarz and Torkian [22] developed two SC systems called artificial neural networks (ANN) Adaptive Neuro-Fuzzy Inference (ANFIS) to estimate the CS of concrete based on several concrete mixed parameters. The study showed that both systems were predicting CS very well. However, the ANFIS model provides slightly better estimates than the ANN model. Another study by [23] presents the ability of both data-driven models, ANN and multiple linear regression (MLR) approaches to predict concrete CS. The study shows that the MLR model has less

prediction accuracy than the ANN model. Moreover, a comparison study has been published between ANN and ANFIS systems to estimate the CS of cement-based mortal materials [24]. The study concluded that the ANFIS faced an overfitting problem and produced undesirable predictions compared to the ANN model. Additionally, Ni and Wang [25] investigate the ability of artificial neural networks (ANN) to predict the CS of concrete. The study revealed that the proposed model provided higher prediction accuracy and could capture the complex relationships between CS and concrete variables.

Another study was conducted by Lee et al. [26] to investigate the potential of using different AI models such as support vector regression (SVR) and ANN models to predict CS of concrete at the age of 28 days. The results showed that SVR predicted CS more accurately than the ANN technique and was less time-consuming. Akande et al.[27] developed two predictive models called ANN and SVR to predict the CS of concrete and concluded that the SVR model was more stable and gave slightly higher prediction accuracy than ANN. Additionally, Ling et al. [28] presented a study to estimate the CS of concrete using a combined model called SVR-CV(SVR is coupled with a cross-validation approach). The proposed model provided a higher accuracy level than other AI models such as ANN and decision tree (DT). Furthermore, satisfactory performance of the ANN model has been noticed throughout the prediction of the CS of high-performance concrete (HPC) and self-compacting concrete (SCC) [29]. Moreover, the feasibility of using the SVR technique and multivariable nonlinear regression (MNR) has been investigated by [30] in terms of the prediction of CS of concrete of lightweight foamed concrete at an earlier age (7-day). The study concluded that the SVR model gives higher estimation accuracy and efficiently captures the non-linear relation between the input variables.

1.4. Hybrid Models. To overcome the issues related to standard models, several scholars have used hybrid AI-based metaheuristic algorithms to enhance the performances of these systems [31, 32]. In literature, several metaheuristic algorithms are employed to optimize AI models such as ANN, SVR, and ANFIS to enhance their performances and obtain much better predictions [10, 33–36]. There is an investigation for accurately predicting the CS of concrete was carried out by Madandoust et al. [37] using adaptive neuro-fuzzy inference systems (ANFIS) and Group method of data handling (GMDH) as a sort of ANN. The GMDH model is enhanced using a genetic algorithm (GA) and singular value decomposition method. The study also conducted sensitivity analyses to illustrate which variables have more effect on CS. The results showed that both adopted approaches could accurately estimate CS at different ages. Besides, another study also conducted a hybrid model carried out by the hybridization ANN with GA to predict CS of concrete in the presence of FA and FS materials [38]. The outcome of the proposed model is validated against the traditional ANN, which is trained by a backpropagation algorithm, and the assessment criteria showed that the hybrid model (ANN-GA) yielded a minor error forecasted than the traditional ANN model. Han et al. [39] presented a hybrid model by combining ANN with particle swarm algorithm (PSO) to constitute the ANN-PSO model to estimate the CS of ground granulated blast furnace slag (GGBFS) concrete. For validation assessment, the performance of the hybrid model (ANN-PSO) is compared with the standard ANN model. The study showed a noticeable improvement in the estimations due to the presence of the PSO algorithm.

1.5. Research Motivation. There is evidence that energy savings, high cement costs, and pressure from environmental organizations and researchers have all led to an increase in the use of industrial waste materials such as fly ash and ground granulated blast-furnace slag in concrete mixing [40]. The use of such materials in concrete makes it more economical and enhances the strength, abrasion, heat evolution, workability, and shrinkage properties of concrete in both fresh and hardened states [41]. Partially replacing cement in concrete mixes is essential because it reduces carbon dioxide emissions into the atmosphere while at the same time lowering the overall cost of producing concrete mixes.

Many researchers proved that it is difficult to provide a consistent method for additive materials (such as fly ash and other cement replacement materials) in the design of concrete mixtures because of the complexity and uncertainty of the design parameters, which significantly influence the compressive strength of concrete. Due to these limitations, engineers in practical use a traditional method called the trial-and-error process to find the right concrete design. However, this approach requires time to accomplish the tests of compressive strength. Thus, applying a fast and efficient method that can predict the compressive strength of concrete immediately or provide the optimal mix design would be very useful. This paper uses artificial intelligence (AI) models to provide an efficient mix-design tool that overcomes these difficulties.

1.6. Research Significance. To the best of the authors' knowledge, no published work in the literature has employed hybrid SVR with GA or improved PSO algorithms to optimize the hyperparameters of SVR for the prediction of CS of concrete with partial cement replacement. The primary advantage of this research is to predict the compressive strength of concrete where the cement was partially replaced with furnace slag and fly ash. Furthermore, the presence of these materials in the concrete mixture makes the relationship between the compressive strength of concrete and other concrete components very complex. Therefore, the traditional modes in such cases could not provide accurate solutions; therefore, thinking of alternative methods having a satisfactory level of flexibility and predictability is vital. Furthermore, in construction and martial fields, accurate prediction of the CS can effectively minimize the costs by reducing the laboratory work and saving time and effort. Accordingly, this study provides an alternative approach to

efficiently estimate one of the most significant features of concrete (CS) in the presence of industrial waste materials. Establishing a systematic approach that can accurately predict the CS of concrete in earlier stages is significant in concrete development and manufacturing because this approach can generate the needed design data faster[42]. Thus, in this study, support vector regression (SVR) combined with two metaheuristic algorithms known as genetic optimizer (GA) and improved particle swarm optimization (PSO) to constitute SVR-PSO and SVR – GA predictive models. The mentioned algorithms optimize the hyperparameters of SVR and kernel parameters and significantly improve the prediction accuracy. Next, the capacities of these models are examined in the case of compressive strength prediction. Accordingly, a powerful AI model called extreme learning machine (ELM) is also prepared and developed for verification purposes. Besides, the performance of the best model is also validated against 14 models developed in previous studies as a crucial step to examine the validity and reliability of the proposed model. Finally, sensitivity analyses are used to identify the most significant parameters that influence concrete CS.

2. Materials and Methods

2.1. Data Collection and Statistical Description. The experimental data used in this current study include seven variables called (Portland cement "ASTM type I"), furnace slag, fly ash (which is produced from the power plant), water, superplasticizer (**C**494[29] **type G**), coarse aggregate (maximum size of 1 cm), fine aggregate (fineness modulus size of 3), and one response variable represent the compressive strength at 28-day age. It is necessary to identify the primary ingredients to understand concrete behavior better. Several considerations should be taken into account through designing the concrete mixes. For instance, More cement content increases the cohesiveness of the mixture, resulting in stickier concrete, and thus cracks may occur. Nevertheless, reducing the cement content considering constant water content results in a mixture with poor cohesion. Therefore, cement content should be optimally assigned to ensure a more reliable concrete mix. On the other hand, the other contents, such as water-cement ratio and fine and coarse aggregate, significantly impact the concrete strength. A very fine aggregate requires more water content to produce a mixture with reasonable consistency. The consequences of increasing the water-cement ratio are significant in reducing the compressive strength of concrete. Therefore, increasing water content usually provides concrete with poor properties. Thus, several researchers have addressed this issue by using chemical additives such as superplasticizers. The primary purpose of conducting these experimental samples is to seek the capability of partially replacing the cement with furnace slag and fly ash. Table 1 presents the statistical description of all data used in this current study. Where Min, Max, Std, and CC symbols in Table 1 refer to the minimum, maximum standardization, and correlation coefficient with the Compressive strength, respectively. The statistical parameters are listed in the table showing a nonlinear relationship between the target and input variables. Moreover, there is a positive relation between cement and fly ash and compressive strength. The cement has the highest correlation with compressive strength with a correlation coefficient (CC) of 0.446, followed by fly ash with a CC of 0.444. The other variables have a negative relationship with CS, and the range of CC is between -0.038 and -0.254.

For better assessing the quality of input parameters mentioned before, their variabilities are statistically compared. As the obtained data have different ranges, the normalization approach is beneficial for enhancing a better perspective. Consequently, all the input parameters and their target are separately normalized between one and zero as follow:

$$x_i' = \frac{x_i - x_{\min}}{x_{\min} - x_{\max}}, \tag{1}$$

where x_i' is the i^{th} normalized value of a variable x.

Figure 1 compares the input variables' variability; therefore, the interquartile ranges (IQR) are calculated using respected quintiles ($Q_{75\%} - Q_{25\%}$). The IQR values of each normalized input variable are given in Figure 1 in the range of 0.274 to 0.650. Superplasticizer with IQR of 0.274) and cement with IQR of 0.641 have the lowest and highest variability compared to other input variables. Lastly, it is essential to mention that the data used in this study is collected from two different sources in the literature and includes 103 data samples [43, 44].

2.2. Genetic Algorithm. Genetic algorithm (GA) is one of the most popular algorithms introduced by John [45] for solving engineering and science optimization problems. This algorithm is inspired by the natural selection theory and then expanded by Goldenberg [46]. GA can find solutions for complex and nonlinear issues, and this aspect is considered one of the main advantages of this algorithm. Different optimization purposes can be addressed by GA, such as continuous or discontinuous or containing a random noise, linear or nonlinear, and static and dynamic. Thus, GA has succeeded in solving optimization problems in various areas. However, it is also characterized as a complicated algorithm because of its limitations, like determining several algorithm parameters (size of population and genetic operator rate) and creating the proper function. Better assigning these parameters is critical for getting highly accurate solutions and having a noticeable influence on the algorithm's convergence; consequently, the designer should be careful [47, 48]. Chromosomes in GA have a fixed length that encodes linear binary strings between 0 and 1. These Chromosomes are significant factors because it is responsible for producing the generations. The chromosome is selected as a random characteristic [49], and the Chromosomes are evaluated according to these characteristics. They are then selected via genetic operators of the remaining Chromosomes and begin producing new generations. Besides, in a range of 0 to 1, crossover selects between parents and mutation work.

Table 1: The statistical description of the used variables in this study.

Variable	Unite	Min	Max	Average	Std	CC
Cement	kg/m^3	137.000	374.000	229.894	78.877	0.446
Slag	kg/m^3	0.000	193.000	77.974	60.461	−0.332
Fly ash	kg/m^3	0.000	260.000	149.015	85.418	0.444
Water	kg/m^3	160.000	240.000	197.168	20.208	−0.254
Superplasticizer	kg/m^3	4.400	19.000	8.540	2.808	−0.038
Coarse aggregate	kg/m^3	708.000	1049.900	883.979	88.391	−0.161
Fine aggregate	kg/m^3	640.600	902.000	739.605	63.342	−0.154
Compressive strength	MPa	17.190	58.530	36.039	7.838	1.000

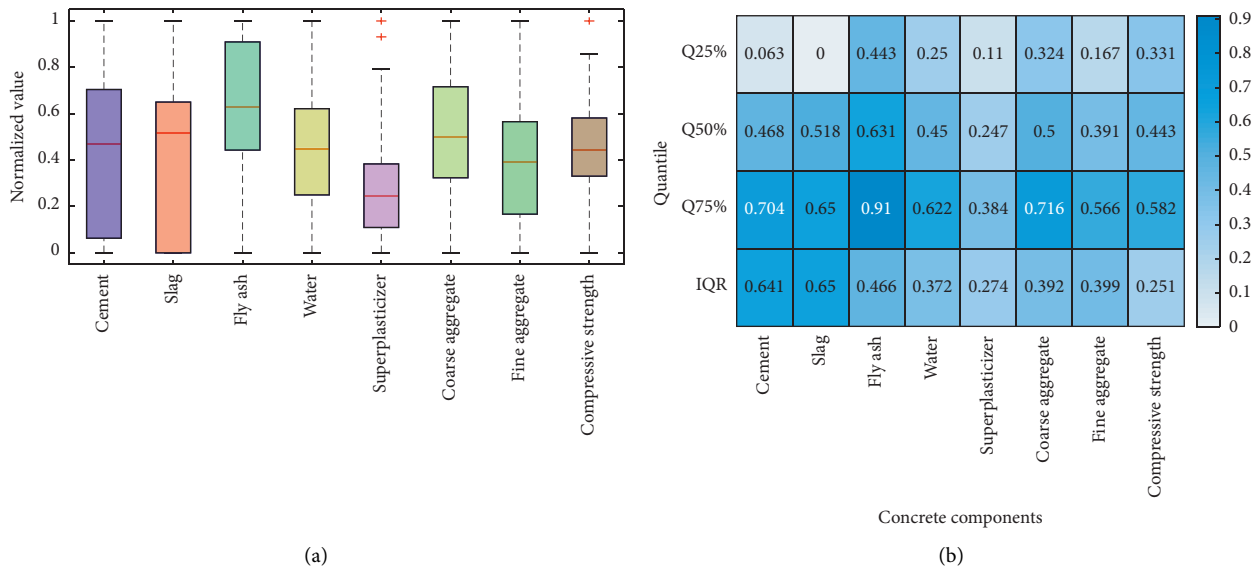

(a) (b)

Figure 1: (a) Boxplot of normalized input and target variables and (b) Quantile percent of the concrete components.

This process is repeated several times until creating the best generations assessed according to their performance [50, 51].

2.3. Particle Swarm Optimization (PSO). The second optimization algorithm used in this study is the PSO algorithm, an approach employed in optimization issues for solution purposes. The PSO algorithm was introduced to the scientific sectors for the first time by Kennedy and Eberhart in 1995 [52], inspired by the accumulative behavior of particles. Less memory required and high learning speed is considered the most compelling characteristic of the PSO compared to GA. The solution of optimization problems in a model based on the PSO algorithm appears like a particle that flies like a bird in the solution space. The framework algorithm of (PSO) is described as follows [53].

Given $x_j^{(i)}$ present the location and $v_j^{(i)}$ is the particle j speed at iteration i, so the following formulas have been utilized to determine the solution for j position and velocity at the following iteration:

$$v_j^{(i+1)} = wv_j^{(i)} + \left(c_1 * r_1 * \left(pbest_j - x_j^{(i)}\right)\right) + \left(c_2 * r_2 * \left(gbest_j - x_j^{(i)}\right)\right), \quad v_{\min} \le v_j^{(i)} \le v_{\max} \ldots, \tag{2}$$

$$x_j^{(i+1)} = x_j^{(i)} + v_j^{(i+1)} = 1, 2, \ldots, n. \tag{3}$$

In the above formula, i represents the number of iterations while w is the coefficient of inertial weight. The rest of the variables are explained as follows:

$pbest_j$: the ideal position for the particles throughout the PSO performance approach.

$gbest_j$: the perfect condition for the particle throughout the PSO performance approach.

r_1, r_2: the arbitrary value in the interval [0,1]. The algorithm of PSO is described as follows:

(i) Set the magnitude of iteration $i = 0$, and for starters, consider an arbitrary location and speed

for the generated particles. Secondly, the structure for every particle has to calculate the value of fitness adjustment.

(ii) Then checking process takes place to compare fitness magnitude with pbest. If the result is improved, the system changes the value of pbest with the new one, leading to an updated magnitude of gbest.

(iii) The PSO approach will calculate the speed value for every particle using equation (2), so the position of every particle will be updated as well using equation (3). Finally, iteration continues by increasing the value of i with $i + 1$ and repeating the process till verification of terminated criteria.

2.4. Support Vector Regression (SVR). In 1995 Cortes and Vapnik [54] developed a technique called Support Vector Machine (SVM) as a form of Artificial intelligence (AI) to deal with classification problems by combining SRM (Structural Risk Minimization) and SLT (Statistical Learning Theory). Consequently, various sectors have commonly employed this technique for regression and prediction problem-solving. The concept of support regression machine (SRM) is the framework of SVM depiction. It presents an effective implementation with high accuracy compared to classical Empirical Risk minimization (ERM), which depends on a conventional learning algorithm, such as neural network techniques. The objective of the SRM is to increase the precision of predicting by minimizing upper and lower limits while reducing training dataset total error is ERM responsibility. Therefore, SVM is considered a practical approach to solving several issues and producing more accurate and reliable predictions [55]. Lately, due to being a more efficient and reliable tool, researchers have been applying SVM in a tremendous section of the prognostication fields conducting various functions related to machine learning [56–60]. Let D denote dataset points $D = \{(x_i, y_i)\} \in R^d * R, i = 1{:}\ n$. The primary concept here is to obtain a function f that contains a connection between x variable and grandeur for determining model y where y is the function of x which is acquired from data D.

$$f(x) = (wx) + b, \quad b \in R, \tag{4}$$

$$f(x) = (w\varnothing(x)) + b. \tag{5}$$

These equations represent linear (4) and nonlinear (5) functions related to regression problems. This approach has involved two stages in obtaining the optimum value for the weight (w) and bias (b). These stages showed applying the Euclidean norm method in the first stage while the second stage presented decreasing produced error magnitude by utilizing empirical risk function. To sum up, minimizing risk function $R_{reg}(f)$ by

$$R_{reg}(f) = R_{emp}(f) + \frac{1}{2}\left\|w^2\right\|. \tag{6}$$

And exhibiting theoretical value empirical error by

$$R_{emp}(f) = C\frac{1}{N}\sum_{1}^{N} L(x_i, y_i, f(x_i, W)), \tag{7}$$

where $L(x_i, y_i, f(x_i, W)$ is the cost function and is derived as one of the two main cost functions used. ε–insensitive loss is the first function, while the second function has been connected with the least square support vector machine (LS-SVM) known as the quadratic loss [61].

Moreover, the equilibrium between empirical risk and the denominated regularization is implied by a regularization constant "C". The following equations present a primer formula for issues of optimization:

$$\min \frac{1}{2}\left\|w^2\right\| + C\sum_{i=1}^{n}(\xi_i + \xi_i^*), \tag{8}$$

$$\text{under the constraints} \begin{cases} y_i - w\varnothing(x) - b \le \varepsilon + \xi_i, \\ y_i - w\varnothing(x) - b \ge -\varepsilon - \xi_i^* \forall_i \in \{1, \ldots n\}, \\ \xi_i, \xi_i^* \ge 0. \end{cases} \tag{9}$$

So, it is more reasonable to consider certain error limits to increase problem solution competence. Therefore, the function accuracy will be approximated where ε indicated a tube size and the slack parameters characterized by ξ_i and ξ_i^*.

The quadratic initiative has been utilized to obtain superior minimized value for regularized risk related to estimating best weight magnitude according to the principle of Lagrange multipliers by implementing optimality constraints [62]. Calculating these multipliers, by using the formula below to the minimum value:

$$\min L(\alpha_i, \alpha_i^*) = -\sum_{i=1}^{n} y_i(\alpha_i - \alpha_i^*) + \varepsilon\sum_{i=1}^{n} y_i(\alpha_i + \alpha_i^*) + \frac{1}{2}\sum_{i=1}^{n}\sum_{j=1}^{n}(\alpha_i - \alpha_i^*)\left(\alpha_j - \alpha_j^*\right)K\left(X_i, X_j\right), \tag{10}$$

as α_i and α_i^* indicate the Lagrange multipliers where $i = 1$ to n at certain limits

$$0 \le \alpha_i, \alpha_i^* \le C, \quad i = 1, \ldots n, \qquad \sum_{i=1}^{n}(\alpha_i - \alpha_i^*) = 0. \tag{11}$$

Finally, a numerical expression for the regression function is described by:

$$f\left(x, \widehat{\alpha_i}, \widehat{\alpha_j^*}\right) = \sum_{i=1}^{n}\left(\widehat{\alpha_i} - \widehat{\alpha_j^*}\right)K(X, X_i) + b^*. \tag{12}$$

The kernel function can be characterized by $K(x_i, x_j) = \varnothing(x_i) * \varnothing(x_i)$ which would have a value depicted by the result of scalar for x_i and x_j vectors in $\varnothing(x_i)$ and $\varnothing(x_j)$ feature space.

One of the main steps to enhance the performance accuracy of the SVR approach is to select the kernel function

properly. The selection process depends mainly on the Mercer conditions [63]. Accordingly, the kernel function type that meets this criterion can be implemented. In this study, the Radial Basis Kernel function (RBF), as expressed below, is used to map the nonlinear relationship between CS of concrete and its dependent variables.

$$K\left(x_i, x_j\right) = \exp\left(-\frac{\left\|x_i, x_j\right\|^2}{2\sigma^2}\right), \tag{13}$$

where σ is the bandwidth of the RBF kernel.

2.5. Extreme Learning Machine. Extreme learning machine (ELM) is an efficient and relatively modern-learning algorithm introduced in 2006 for training feedforward neural network (FFNN) instead of the conventional algorithm (i.e., backpropagation algorithm). The ELM model is the same as the structure of a single layer of FFNN, including three critical layers (input, hidden, and output). ELM has many advantages that surpass its counterpart FFNN, including speed and well generalization abilities [63, 64]. Moreover, the traditional FFNN has many defects and shortcomings, including low convergence, local minima problems, overfitting, and poorer generalization. Furthermore, classical FFNN is usually trained using a backpropagation algorithm, and hence, it becomes more likely to be stuck into local minima.

The structure of the ELM model consists of three successive layers called input, hidden, and output layers, respectively. The input layer receives the predictor vectors, while the hidden layer contains several hidden nodes to process the data to the output layer. It is important to say that data transmission from layer to next layer through neurons. Lastly, the output layer is responsible for producing the calculated outcomes of the model. The hidden layer is essential because it contains the majority of the information of the data.

The core concept of ELM is the weights and bias values used to link the transmission data from the input layer to the hidden layer. These values are assigned randomly and do not need to be corrected. Therefore, this algorithm is very fast. Then, the activation function is usually nonlinear applied to extract the most significant features from data which will be passed to the next layer. It is essential to mention that the output layer weights are calculated based on Moore–Penrose approach [65].

The steps below show the process of establishing the ELM model.

(i) Inputting the predictors and their corresponding targets (output values).

(ii) Defining the number of hidden nodes in the hidden layer using the trial-and-error procedure.

(iii) Assigning the weight and bias values of the hidden layer randomly.

(iv) Data normalization.

(v) Selecting transfer function.

(vi) Processing the data in hidden nodes using equation (14) to prepare it for the next layer (calculating the output of hidden layer H).

(vii) Determining the output layer weights using the Singular Value Decomposition (SVD) approach as shown in equations (15) and (16).

(viii) Computing the predicted targets (CS).

(ix) Denormalizing predicted targets (CS).

$$H(x, \alpha, \beta) = \begin{bmatrix} g(x_1) \\ . \\ . \\ . \\ g(x_N) \end{bmatrix} = \begin{bmatrix} g(a_1.x_1 + \beta_1) \ldots g(a_L.x_1 + \beta_L) \\ . \\ . \\ . \\ g(a_1.x_N + \beta_1) \ldots g(a_L.x_N + \beta_L) \end{bmatrix}, \tag{14}$$

where g is the activation function, x, β, a respectively are the input vectors, bias, and weight values.

$$HB = Y. \tag{15}$$

Then, calculate the output weights from equation (16)

$$\widehat{B} = H^{\dagger}Y, \tag{16}$$

where $H^{\dagger}$ denotes the Moore-Penrose generalized inverse of Hussain matrix, Y is the actual targets, and B is the vector that contains output weights calculated by the SVD method. It is essential to mention that the sigmoid transfer function is used as an activation function in the hidden layer.

2.6. Hybrid Models: Model Development. The SVR algorithm usually uses a specific kernel function to calculate the hyperplane to fit the data well. The majority of engineering issues are very complex. Therefore, it is beneficial to use the nonlinear kernel function, and hence there will be three most efficient hyperparameters (C, ε, and γ) of the SVR approach that greatly influence the SVR performance. The gamma parameter (γ) increases the algorithm's capability to match the training data ideally with their corresponding target(s), while the cost parameter (C) is a penalty metric for promoting the process of predicting the data instances more correctly. Decreasing the value of γ ($1/2\sigma^2$) would negatively affect SVR performance and thus, underfitting the data; however, increasing too much gamma results in overfitting the dataset. Consequently, the optimal values of these hyperparameters (C, ε, and γ) significantly impact the SVR performance, thereby getting more accurate predictions.

In the literature, there are several attempts to select these hyperparameters of SVR. One of these strategies, using trial and error methods. However, this approach may not provide the optimal solutions as it is also limited in a specific range of assumptions. Moreover, this approach is time-consuming and requires a higher computational cost. The other procedure to compute the hyperparameters of SVR is called grid -search approach. This strategy also has several disadvantages, such as required computational efforts and time. In

addition, this strategy requires a limited range of assumptions of each parameter; it sometimes gives some of the hyperparameters less attention than others. Thus, in this study, these hyperparameters are efficiently optimized using two different optimizations, namely, genetic and particle swarm algorithms. Figure 2 and Figure 3 show the incorporation of SVR with these algorithms [66, 67]. The root mean square error formula is used as a fitness function of both algorithms.

The main steps regarding the hybridization of SVR (calibration processes) are stated below:

(i) Dividing data into sets, training (75%; 77 samples), and testing set (25%; 26-sample).

(ii) The training set data is used to develop SVR-GA and SVR-PSO models.

(iii) Selecting the root mean square error as an objective function.

(iv) Initializing the parameters for each algorithm (GA and PSO).

(v) Defining the range of each hyperparameter. In this study, the algorithms first search these parameters from 0 to 1.

(vi) As some hyperparameters such as C have a wide range of data (from 0 to infinity), we reconstruct this obtained value from the previous step as $C = 1/c$, where C is obtained from the previous step.

(vii) The algorithm starts finding the optimal parameters that reduce the objective function (in this study, RMSE is used as an objective function).

(viii) The applied algorithm has been given a significant task to increase the accuracy during the calibration process by minimizing the cost function.

(ix) In this study, the cost function is described as root mean square error (RMSE = $\sqrt{(1/N)\sum_{i=1}^{N}(CS_{obs_i} - CS_{pred_i})^2}$).

(x) The algorithm then starts using random numbers to assign the hyperparameters and updates these values until optimal accuracy or maximum iteration is achieved.

(xi) Inserting the reconstructed hyperparameters to the SVR algorithm.

(xii) Calculating the other SVR parameters like beta and alpha using minimal sequential optimization (SMO) is considered a more efficient algorithm [68].

(xiii) Calculate the cost function (RMSE).

(xiv) If the RMSE is very small or the algorithm reaches the maximum iterations, the algorithm stops the calibration process. Otherwise, the applied algorithm continues the updating of hyperparameters.

It is essential to mention that all predictive models used in this study are developed using MATLAB 2018b.

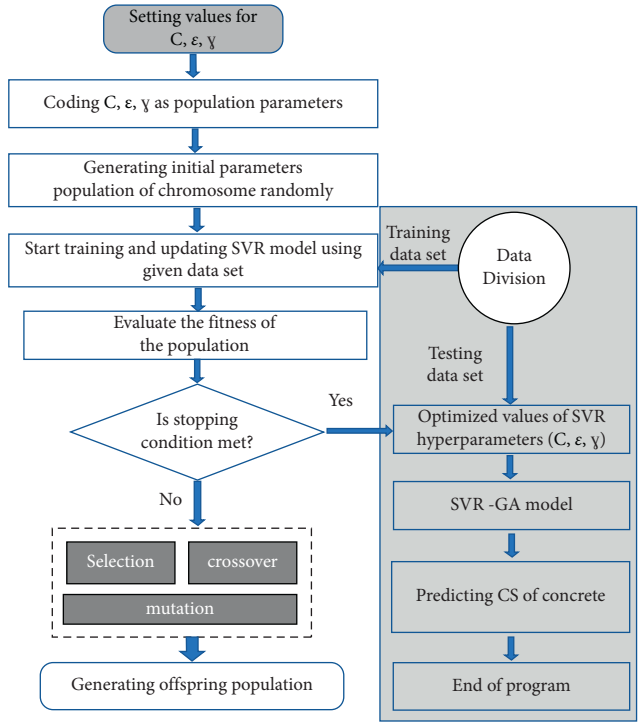

Figure 2: Incorporation of SVR with genetic algorithm.

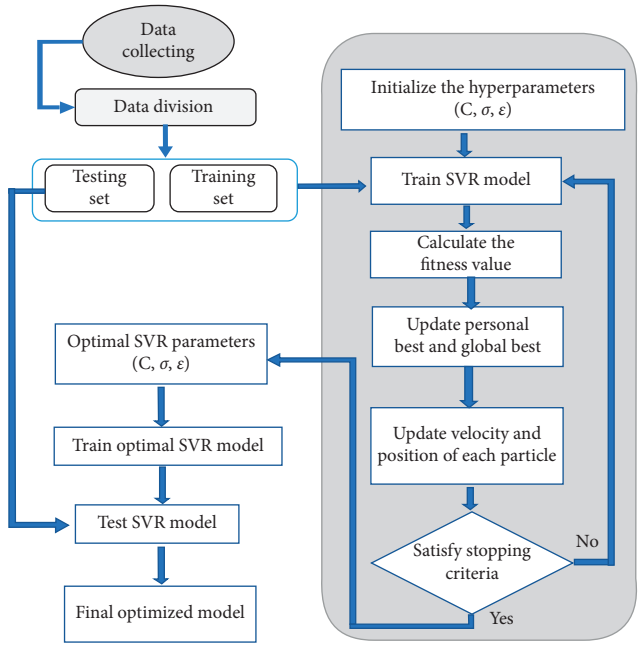

Figure 3: Incorporation of SVR with the genetic particle swarm algorithm.

Concerning PSO, it is used based on the algorithm described in Kennedy and Eberhart [52], with some modifications and improvements suggested by Pedersen [69] and Mezura-Montes and Coello Coello [70].

2.7. Statistical Matrices. In this paper, nine parameters accounting for the error between measured and predicted CS of concrete is used, namely; mean absolute relative error (MARE), root mean square error (RMSE), mean absolute error (MAE), maximum absolute percentage relative error (erMax), uncertainty at 95% (U95), correlation of coefficient (CC), correlation of determination (R^2), Nash–Sutcliffe model efficiency coefficient (NE), Index of Agreement or Willmott (WI), and relative error (RE). Some of the stated parameters like R^2, CC, NE, and WI measure the strength of the relation between predicted and actual vectors, usually having values in the range of 0 to 1. On the other hand, the error metrics like RMSE, MARE, MAE, erMax, U95 measures are used to compute the forecaster error. The best model should provide fewer values of error measures (as lower as possible) and the highest value of correlation measures (near to one). In this study, the U95 parameter is used to efficiently select the best model accuracy when some of the proposed models would give close estimates of CS of concreter, and hence it would be challenging to choose the best predictive model. Some earlier studies showed that the U95 could help in the detection of the statistical differences between outcomes of comparable models and the actual values much better than other statistical parameters such as RMSE, MAE, R^2, and so on [63]. Furthermore, the a-20 index as a new engineering metric is used to further assess the applied models' performances. It is essential to mention that the perfect and ideal model has a-20 index of 1. The a-20 index has an essential advantage in the engineering field because this factor quantifies the number of experimental samples that satisfy the predicted magnitudes with a deviation of ±20%, compared to the corresponding (experimental) values [71].

The mathematical expressions of these statistical parameters are derived from equations (17) to (26) [72, 73].

$$\text{MARE} = \frac{1}{N}\sum_{i=1}^{N}\left|CS_{obs_i} - CS_{pred_i}\right|, \tag{17}$$

$$\text{RMSE} = \sqrt{\frac{1}{N}\sum_{i=1}^{N}\left(CS_{obs_i} - CS_{pred_i}\right)^2}, \tag{18}$$

$$\text{MAE} = \frac{1}{n}\sum_{t=1}^{n}\left|CS_{obs_i} - CS_{pred_i}\right|, \tag{19}$$

$$CC = \frac{\sum_{t=1}^{n}\left[\left(CS_{obs_i} - \overline{CS_{obs_i}}\right)\left(CS_{pred_i} - \overline{CS_{pred_i}}\right)\right]}{\sqrt{\sum_{t=1}^{n}\left(CS_{obs_i} - \overline{CS_{obs_i}}\right)^2 \sum_{i=1}^{n}\left(CS_{pred_i} - \overline{CS_{pred_i}}\right)^2}}, \tag{20}$$

$$\text{erMAX} = \max\left(\left|\frac{CS_{obs_i} - CS_{pred_i}}{CS_{obs_i}}\right|\right), \tag{21}$$

$$\text{U}_{95} = 1.96\left(\text{SD}^2 + \text{RMSE}^2\right)^{1/2}, \tag{22}$$

$$R^2 = 1 - \frac{\sum_{i=1}^{n}\left(CS_{obs_i} - CS_{pred_i}\right)^2}{\sum_{i=1}^{n}\left(CS_{pred_i} - \overline{CS_{pre\ d}}\right)^2}, \tag{23}$$

$$\text{WI} = 1 - \frac{\sum_{i=1}^{n}\left(CS_{obs_i} - CS_{pred_i}\right)^2}{\sum_{i=1}^{n}\left(\left|CS_{pred_i} - \overline{CS_{obs}}\right| + \left|CS_{obs_i} - \overline{CS_{obs}}\right|\right)^2}, \tag{24}$$

$$NS = 1 - \frac{\sum_{i=1}^{n}\left|CS_{obs_i} - CS_{pred_i}\right|}{\sum_{i=1}^{n}\left|CS_{obs} - \overline{CS_{obs}}\right|}, \tag{25}$$

$$\text{RE}\% = \frac{CS_{obs_i} - CS_{pred_i}}{CS_{obs_i}} * 100, \tag{26}$$

$$a20\ \text{index} = \frac{m20}{n}, \tag{27}$$

where CS_{obs_i} and CS_{pred_i} are respectively observed and predicted value of i-th sample; CS_{obs}, and CS_{pred_i} are the average of observed and predicted values separately. While n refers to the total number of samples, and $m20$ refers to the number of samples with an experimental rate value/predicted value between 0.80 and 1.20. Lastly, SD is the standard deviation of the forecasted errors.

3. Results and Discussion

Compressive strength (CS) of ordinary and high-strength concrete is a significant property during manufacturing the cement. Many factors affect CS, and the relationship between them and CS of concrete is highly nonlinear for classical and high strength concrete. This part of the study discusses the calculated results obtained by three different models, ELM, SVR-GA, and SVR-PSO.

Table 2 provides more information regarding the performance of each predictive model during the training phase. At first glance, the hybrid model (SVR-GA and SVR-PSO) provided much more accurate predictions than the ELM model. Moreover, the ELM could not recognize very well the complex relation between CS and its' factors thereby decreasing the accuracy and increasing the forecasting errors (MAE = 1.890, RMSE = 2.614, MAPE = 0.054, CC = 0.939, U_{95} = 370.638, NE = 0.883, WI = 0.968, a20-index = 0.974 and erMax = 0.212). However, the other both models (SVR-GA and SVR-PSO) gave high accurate forecasting in addition to a slight preference in favor of SVR-GA model (MAE = 0.673, RMSE = 1.011, MAPE = 0.021, CC = 0.993, U_{95} = 6.882, NE = 0.982, WI = 0.995, and erMax = 0.102).

The quantitative assessment is in Table 2 illustrates that the SVR-PSO model can predict CS of concrete at a good

Table 2: Assessing the performance of each suggested model: training set.

Model/statistical measures	SVR-PSO	SVR-GA	ELM
MAE (MPa)	0.978	**0.673**	1.890
RMSE (MPa)	1.163	**1.011**	2.614
MAPE (MPa)	0.028	**0.021**	0.054
CC	**0.997**	0.993	0.939
U_{95}%	**6.107**	6.882	370.638
NE	0.977	**0.982**	0.883
WI	0.994	0.995	**0.968**
erMax	**0.065**	0.102	0.212
*a*20-index	**1**	**1**	0.974

Bold values represent the higher accuracy value.

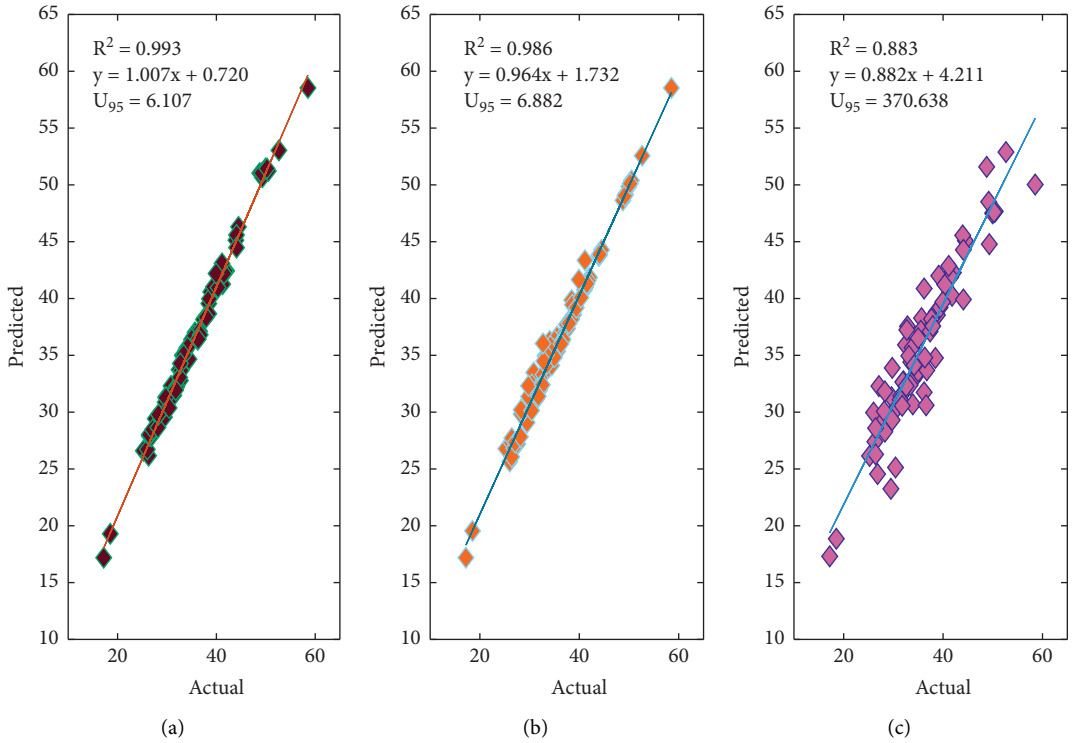

Figure 4: Comparing between actual and predictive values: correlation of determination, a, b, and c are respectively referring to SVR-PSO, SVR-GA, and ELM.

level of accuracy with MAE of 0.978, RMSE of 1.163, MAPE of 0.028, CC of 0.997, U_{95} of 6.107, NE of 0.977, WI of 0.994, and erMax of 0.065. Finally, the most important note that can be drawn based on the given outcomes is that the differences between the performances of the applied three modes under statistical measures, in general, are minimal except the given assessments obtained from the U_{95} parameter.

As shown in Figure 4, scatter plots prove helpful information on the performance of each adopted model by explaining the diversion of every predicted point to the actual value. According to the figure, it can be shown that the SVR-PSO model is considered the best model in the prediction of CS of concrete and provides the highest R^2 (0.993), followed respectively by the SVR-GA with R^2 of 0.986 and ELM with R^2 of 0.883. Moreover, the predicted values obtained by the SVR-PSO model are found to have less dispersion and sticker to the fitted line than other comparable models (i.e., ELM and SVR-PSO).

Although the SVR-GA and SVR-PSO provided the highest prediction accuracies compared to the ELM model, very few statistical differences were found between their performances, and the training set could not give a robust assessment as the models were trained based on known targets. Therefore, the testing phase is crucial in assigning the best predictive models for CS of standard and high strength of concrete. At the testing phase, the model would assess under unknown targets. Thus, the generalization capabilities of each adopted model can be revealed [74]. Several

Table 3: Assessing the performance of each suggested model: testing set.

Model/statistical measures	SVR-PSO	SVR-GA	ELM
MAE (MPa)	1.101	2.008	1.657
RMSE (MPa)	1.386	2.826	2.180
MAPE (MPa)	0.034	0.067	0.047
CC	0.989	0.956	0.965
U_{95}%	28.776	518.686	183.182
NE	0.972	0.883	0.930
WI	0.992	0.962	0.981
erMax	0.151	0.417	0.175
a20-index	**1**	**0.923**	**1**

Bold values represent the higher accuracy values.

statistical metrics are tabulated in Table 3 to evaluate the proficiency of the proposed models. Following statistical metrics, the SVR-PSO is found to have the highest accuracy of prediction with the fewest metrics errors (MAE = 1.101, RMSE = 1.386, MAPE = 0.034, CC = 0.989, U_{95} = 28.776, NE = 0.972, WI = 0.992, and erMax = 0.151). Based on the same table, the forecasted error increased in related to applying SVR – GA of estimation CS during tidying set (MAE = 2.008, RMSE = 2.826, MAPE = 0.067, CC = 0.956, U_{95} = 518.686, NE = 0.883, WI = 0.962, and erMax = 0.417). The presented results explain the ELM model's performance gives much better predictions than the SVR-GA model with MAE of 1.657, RMSE of 2.614, MAPE of 0.047, CC of 0.956, U_{95} of 183.182, NE = 0.930, WI of 0.981, and erMax of 0.175.

The presented statistical parameters indicate that all used models except SVR-PSO gave relatively higher errors in the testing phase than their training performance. As a result, the SVR-GA and ELM models have faced overfitting issues. The other most significant observation extracted from the statistical description shown in Table 3 is that the statistical metric (U_{95}%) is the most efficient parameter in determining the best accuracy model. The importance of that parameter appears in selecting the highest quality model among several modeling techniques when the values of other statistical indicators are much closer to each other and no significant differences are noticed. Thus, the SVR-PSO model performs superior to all comparable models.

As the testing part is very significant, visualization assessments are excessively used to identify the best model's capacity and verify whether the SVR – PSO still outperforms other used techniques according to visual assessments. As illustrated in Figure 5, the scatter plots clearly showed that the SVR – PSO model is closer to the actual CS of concrete than other used models. The given results indicated a higher accuracy prediction of CS than other models. Moreover, the SVR-PSO model recorded the highest value of R^2 of 0.978 followed by SVR – GA (R^2 = 0.931), and ELM (R^2 = 0.914). Despite the SVR-GA provider higher value of R^2 than the ELM model, it produces very high uncertainty compared to the ELM technique. In order to obtain adequate and informative graphical evaluation error forecasting, relative error, as shown in Figures 6(a)–6(c), is established for exhibiting the relative error (RE %) for every sample over the testing set. The figure can also give a better understanding of the model's efficiency in predicting CS for every single sample. It can be observed that the proposed SVR – PSO generates the fewest RE% values compared to the other modeling approaches. The average absolute relative error for the SVR – PSO model was recorded significantly fewer (3.40%) compared to other models ELM (4.74%) and SVR-GA (6.71%), respectively.

Moreover, the distribution of RE% for each suggested model is plotted in Figure 6(d). The boxplot presentations are created to evaluate the suggested models' performances and illustrate the visualized information regarding the efficiency of the models in predicting the CS of standard and high strength concrete. The comparable models (SVR-GA and ELM) generated undesirable outlier values with a relatively higher interquartile range (IQR). However, the SVR-PSO model performance is excellent. The estimates were noticed to have the fewest extreme values compared to adopted models. Moreover, the predicted median of RE% obtained by the SVR-PSO model was nearest to zero. Concerning interquartile range (IRQ), the proposed model (SVR-PSO) predicts a more desirable value of IRQ (5.235) compared to SVR-GA (6.662) and SVR-PSO (7.439).

Furthermore, Table 4 is created based on the predicted compressive strength of concrete values using the applied models during the testing phase. It shows that the SVR – GA model sometimes provides estimates with higher errors than the other models. For instance, the difference between the experimental value and predicted value in sample 19 was noticed to be very high (8.08 MPa). Furthermore, the other vital observation that can be concluded from that table is that the applied model (PSO – SVR) generates very accurate predictions for CS of high and normal strength of concrete. It can be said that (PSO – SVR) models are more efficient for predicting the cs in the presence of waste industrial material in the concrete than the SVR – GA and ELM. Moreover, Figure 7 provides more information about the efficiency of the predicted models during the testing phase. Based on that figure, the estimated values by the SVR-PSO model are very accurate and closer to their corresponding observations.

In order to evaluate the performances of all suggested models more efficiently, the Taylor diagram, as shown in Figure 8, is created based on the outcomes of each predictive model developed in this study during the testing phase. In this figure, both axes (vertical and horizontal) are connected via a circular line, representing the standard deviation. The value of the coefficient of correlation as a performance indicator is indicated by the black radial lines drawn from the center of the coordinates, and the circular walnut lines indicate the value of root mean square error (RMSE) and another significant performance indicator. In this figure, the actual dataset is placed in the base of the Taylor diagram and assumes that the data have the highest correlation of coefficient (i.e., CC = 1), RMSE of zero, and a calculated standard deviation (SD) value. Then, the performances of each model in terms of the three statistical parameters (RMSE, CC, and SD) are compared with those evaluated from the actual dataset. Thus, the efficiency of the predictive modeling approach can be easily identified via assessing its

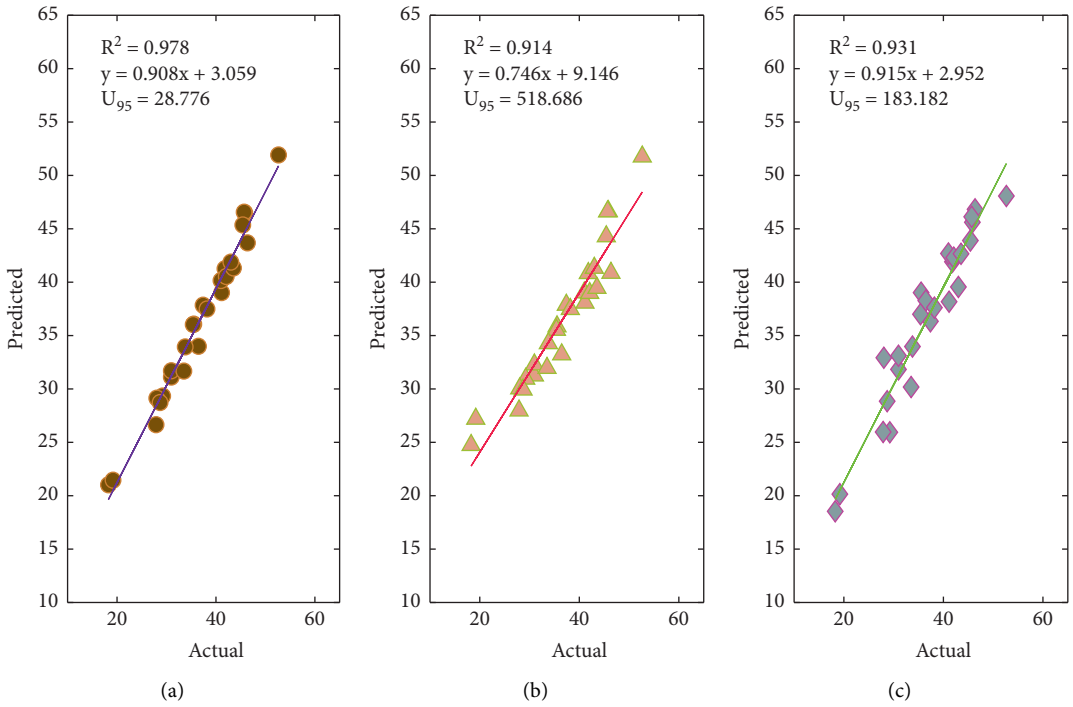

Figure 5: Comparing between actual and predictive values: correlation of determination, (a, b, and c) respectively belong to SVR-PSO, ELM, and SVR-GA.

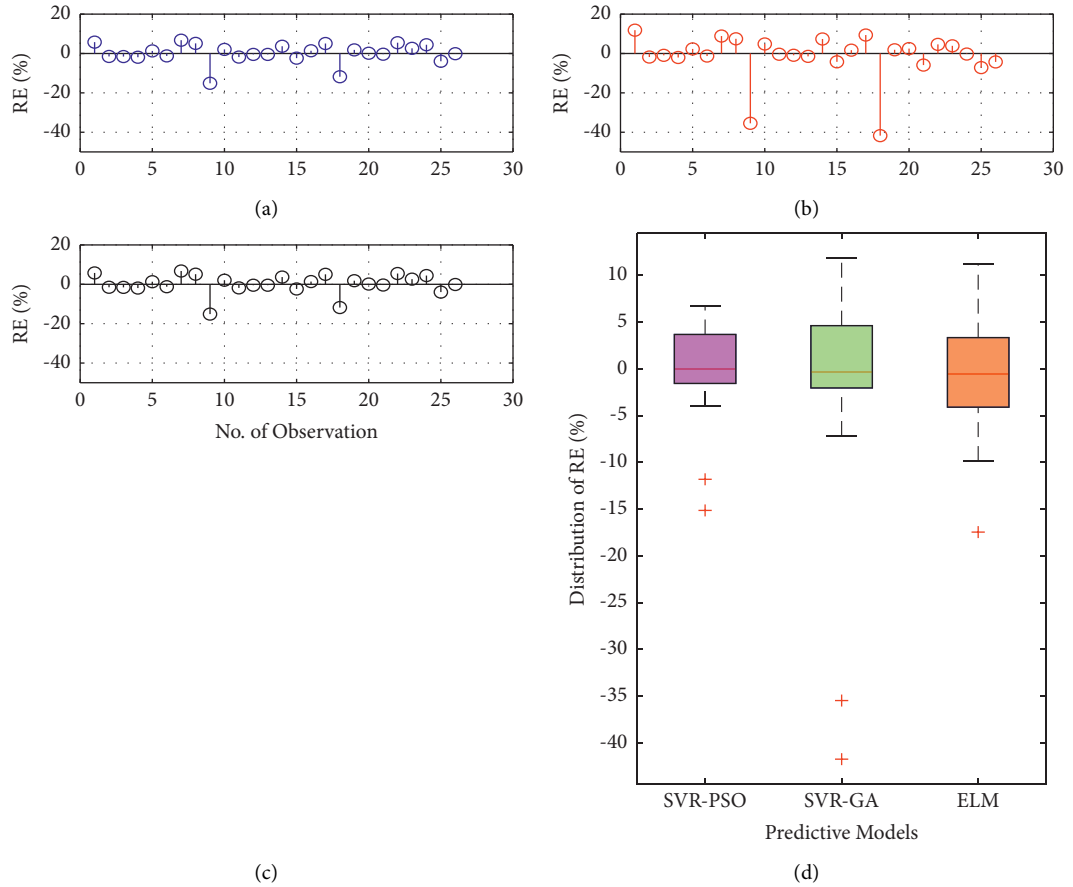

Figure 6: Comparison of the performances of three adopted models: (a, b, and c respectively belong to SVR-PSO, SVR-GA, and ELM, while d shows the boxplot presentation for illustrating the distribution of relative error for all adopted models in a single plot.

Table 4: The predicted compressive strength values using applied models versus the experimental values during the testing phase.

No. Sample	SVR-PSO (MPa)	SVR-GA (MPa)	ELM (MPa)	Experimental (MPa)
1	28.73	29.93	28.85	28.70
2	36.07	35.85	39.02	35.52
3	46.56	46.62	46.12	45.69
4	41.26	40.84	41.91	41.81
5	37.85	37.87	36.34	37.39
6	34.00	33.23	38.27	36.46
7	39.03	38.07	38.17	41.14
8	21.02	24.74	18.54	18.26
9	40.16	39.03	42.69	41.01
10	36.03	35.53	37.00	35.39
11	31.11	31.25	31.83	30.97
12	43.68	40.87	46.82	46.36
13	33.94	34.27	33.97	33.78
14	40.53	38.98	42.30	42.08
15	31.70	32.28	33.11	30.97
16	46.51	46.64	45.61	45.82
17	51.92	51.76	48.07	52.65
18	41.33	39.46	42.66	43.54
19	21.46	27.20	20.15	19.19
20	37.49	37.47	37.62	38.19
21	45.36	44.29	43.90	45.42
22	29.34	30.95	25.94	29.23
23	31.67	31.96	30.18	33.51
24	41.88	41.33	39.55	43.01
25	26.65	27.97	25.97	27.89
26	29.14	30.04	32.92	28.03

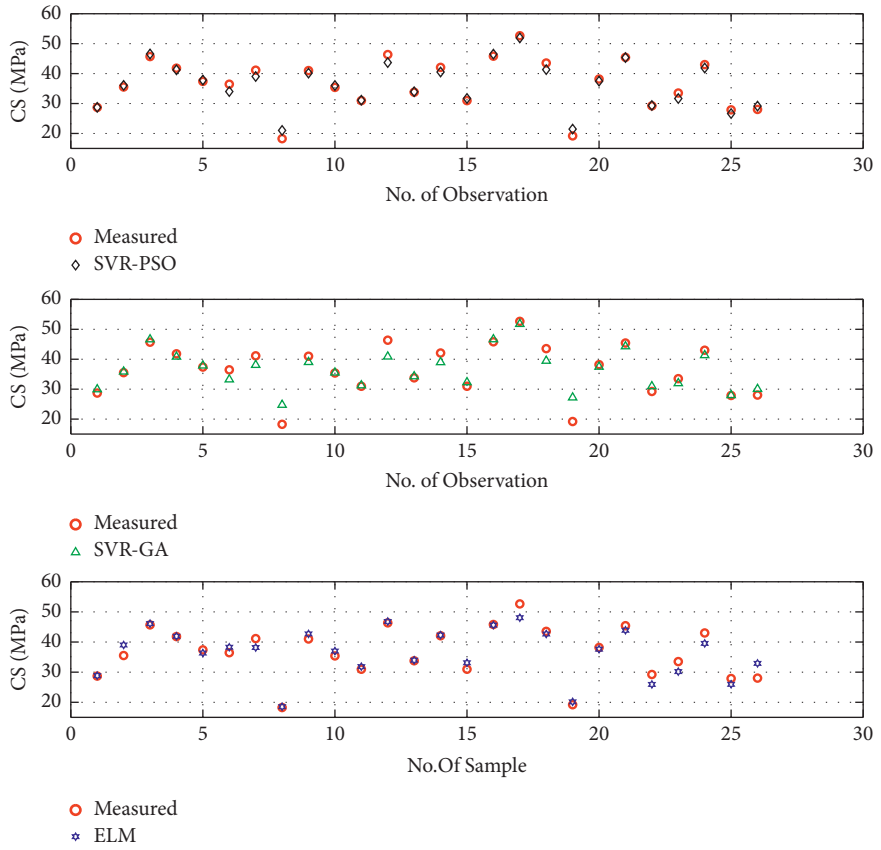

Figure 7: Comparison between the measured compressive strength of concrete and the predicted values.

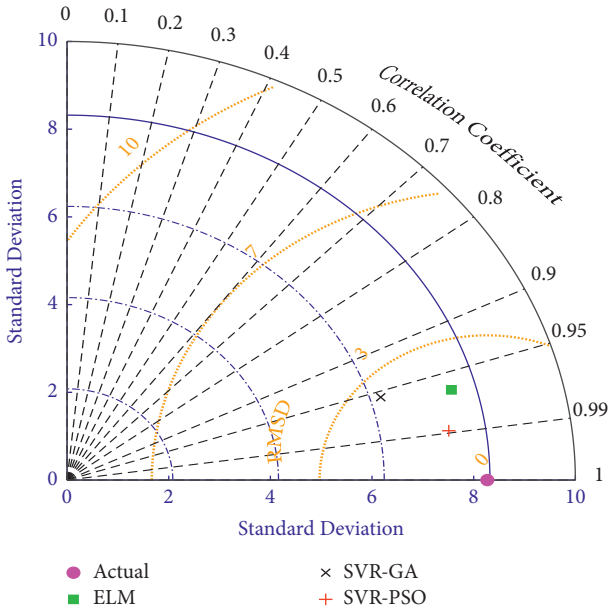

Figure 8: Taylor diagram for comparing the performances of the proposed models: testing set.

similarity with the based model of the actual dataset. It can be seen from this figure that the SVR-PSO model takes the closest position to the actual data, which indicates the excellent performance of this model. However, the other models (SVR-GA and ELM) show a lower similarity with the actual data than the SVR-PSO model during the testing phase.

Finally, both quantitative and visualized assessments referred to the adopted predictive model (SVR-PSO) have performed very well in training and testing phases to predict the compressive strength of standard and high-performance concrete. Although the CS has had a complex relationship with the existing parameters, the proposed modeling approach was very stable and gave the highest accuracy results compared to other comparable models. For ensuring the reliability of the proposed model (SVR-PSO), the outcome of this model during the testing set will be compared with other predictive models conducted in previous studies in terms of coefficient of determination (R^2). This indicator is very efficient when comparing a specific model's outcomes to others developed in other studies with a different dataset. The most important thing is that this parameter is not affected by normalization and the scale of the dataset. The models are developed based on a given dataset from different ranges and distributions. However, most other statistical criteria such as RMSE, NSE, and other criteria are mainly influenced by the scale of the used data set. When comparing different predictive models established from several datasets, these parameters may be misleading. Finally, the hyperparameters of SVR, which PSO and GA have optimized, are presented in Table 5.

3.1. Comparing the Proposed Model with Others Developed in Previous Studies. Shariati et al. [10] presented a novel model by incorporating the extreme learning machine and grey wolf optimizer to predict the concrete CS. For

Table 5: The optimized hyper-parameters of SVR by PSO and GA.

Parameter	GA	PSO
C	1.160329	8.511694
γ	$8.007E-03$	0.015044
ε	0.990097	0.048581

compression purposes, the authors used standard extreme learning machine (ELM), support vector regression (SVR) with different kernel functions, artificial neural network, and adaptive neuro-fuzzy inference system (ANFIS). The assessment results revealed that the proposed modeling approach outperformed other modeling approaches with desirable accuracy ($R^2 = 0.9381$). Another study [75] investigated using the data mining approach as a computer aid to predict CS of high-strength concrete. The authors used a cross-validation (CV) approach with a multiple additive regression tree (Mars). The proposed model is evaluated with other approaches like ANN and SVR, statistical model, and bagging regression trees. The results discovered that the comparable models gave undesirable performances while the proposed model achieved the highest accuracy with R^2 of 0.943. The study conducted that the other modeling approaches gave lower accuracy and suffered overfitting problems. Chou et al. [27] applied two approaches to estimate concrete CS, called ANN and SVR. In order to achieve better performances, the authors developed both models using the same dataset. However, the performance of the ANN model was slightly lower than the SVR model. The study concluded that the SVR is more stable and hence gives the higher prediction accuracy with R^2 of 0.9551. Moreover, Pham et al. [76] investigated the hybridization of least square support vector regression with a firefly algorithm to establish a hybrid model called (LS-SVR-FFA) for predicting CS of high-performance concrete. For verification of the performance of the hybrid model, authors used other benchmark models called SVR and ANN. the results found that the LS-SVR-FFA model was very accurate compared to SVR and ANN models in the prediction of CS of concrete with R^2 of 0.89. Bui et al. [77] hybridized the novel whale optimization algorithm with the ANN approach to enhance the model's performance in predicting concrete CS. The authors also incorporated the neural network with several algorithms (ant colony optimization and dragonfly algorithm). The outcomes of the study showed that the proposed model (WOA-NN) gains the fewest error forecasting and best performance (R^2 = 0.898). Another study was conducted by Hameed and AlOmar [4] to predict CS of concrete using the ANN-CV model. The study used the multiple linear regression (MLR) model for comparison and validation of the performance of the proposed model. The study concluded that the MLR approach could not provide desirable results as ANN models though using CV techniques with both models. However, the superiority of the ANN model is obvious in terms of accuracy performance (R^2 = 0.931). Table 6 provides more reverent studies which developed different prediction models for the prediction of CS of concrete. Based on the outcome of the reviewed models collected

Table 6: Validating the SVR – PSO against predictive models collected from the literature.

Reference	Model	R^2
[10]	ELM-GWO	0.9381
[75]	MART-CV	0.943
[27]	SVR	0.9551
[76]	LS-SVR-FA	0.89
[77]	WOA-ANN	0.898
[4]	ANN-CV	0.931
[78]	MARS-GBM	0.956
[79]	ANN	0.922
[80]	Neural-expert system(NEX)	0.76
[81]	Fuzzy polynomial neural networks (FPNN)	0.821
[82]	ANN	0.934
[83]	EFSIM	0.927
[84]	RELM- CV	0.884
[85]	XGBoost with feature selection	0.9339
Proposed model (SVR-PSO)		**0.978**

from the literature, the suggested model (SVR-PSO) outperformed all comparable models developed and used in previous studies.

3.2. Sensitivity Analysis. After assessing the reliability of the proposed model (SVR-PSO) and validating its performance against different models developed in previous studies to predict CS of concrete, it is vital to conduct sensitivity analyses to identify the most significant parameters that have an important influence on CS of concrete. Moreover, the selection of the most influential parameters has great importance in minimizing time and cost as well as this step is vital in structural and material engineering [86]. The cosine amplitude method is applied in this current paper [47, 87]. The mathematical expression of the amplitude method can be seen according to the following equation:

$$R_{ij} = \frac{\sum_{k=1}^{n}\left(X_{ik} * X_{jk}\right)}{\sqrt{\sum_{k=1}^{n} X_{ik}^2 \sum_{k=1}^{n} X_{jk}^2}}, \tag{28}$$

where R_{ij} is the correlation degree between each input variable and target (CS of concrete). This factor ranges between 0 and 1. If there is a high correlation between a parameter with CS of concrete, the value of R_{ij} is becoming close to one. On the other hand, if there is no relation between a variable and CS of concrete, the value R_{ij} equals zero. Moreover, in the stated equation, n is the number of samples during the crucial step of this study (i.e., testing set), and the parameters X_i and X_j, respectively are the input and output values (CS of concrete). Figure 9 shows the influence of each used parameter on the CS of concrete. It found that the fine aggregate, coarse aggregate, water, and cement variables have the highest impact on CS. However, the other input parameters (i.e., SP, fly ash, and slag) have a lower impact on the CS of concrete.

3.3. Limitation of the Proposed Method and Possible Future Research. The obtained results have proved the capability of SVR-PSO in the prediction of CS of concrete where the cement was partially replaced with other materials. The

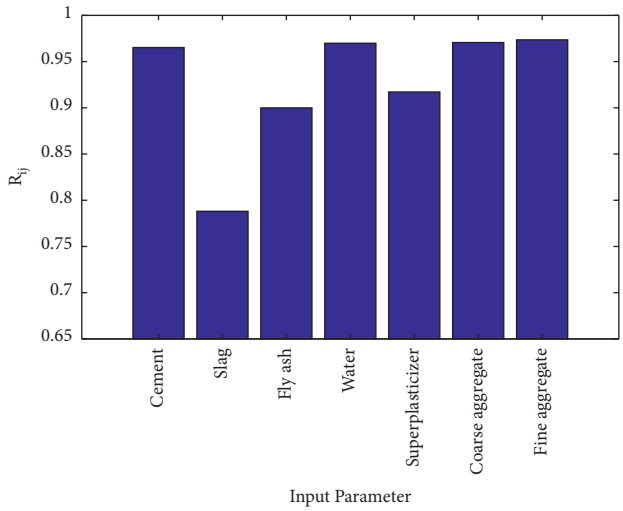

Figure 9: Sensitivity analysis results.

proposed model showed an important improvement in prediction capacity compared to other comparable models such as ELM and SVR-GA. Besides, the input predictors of this study, including seven different materials, are introduced to the models to predict the CS property. However, the prediction accuracy of the proposed model may improve if the advanced data preprocessing technique is applied. Moreover, the input vectors may have uncertainties and are correlated, which eventually hider the model's performance. Therefore, this study recommends applying the principal component analyses (PCA) approach before training the model. Applying the PCA approach has a significant advantage in eliminating the redundant information and correlation between input data, thereby enhancing the predicting accuracy of the applied model.

4. Conclusions

The significant contribution of this research was to develop a hybrid AI model for the prediction of compressive strength of concrete with 28-day age where the cement was partially replaced with the pozzolan powders such as furnace slag and fly ash. The traditional approaches such as the trial-and-error method applied to find the optimal concrete design have some limitations since the process is time-consuming and needs several experimentals. Furthermore, the process of partially replacing cement in concrete manufacturing makes the relationships between CS and concrete components very complex. Accordingly, the classical method does not provide the most optimal solutions. Thus, this research has introduced a novel approach as an efficient and cost-effective method to early estimate the CS. For this regard, SVR is hybridized with two different nature-inspired optimizations like modified PSO and GA, constituting SVR-PSO and SVR-GA models, respectively. These algorithms are given a significant task in optimizing the hyperparameters of SVR. Furthermore, the ELM model is also developed for validating the performances of both SVR-PSO and SMR-GA. There were eight statistical matrices used for assessing

the performance of each model separately. The results showed that all proposed models (ELM, SVR-GA, and SVR-PSO) provided good estimates. However, there were significant differences reported throughout the testing set. Additionally, the reported results uncovered that the SVR-GA suffered overfitting problems. Although the ELM model has been found to provide highly accurate estimates compared to the SVR-GA model, the SVR-PSO model was superior in predicting the compressive strength of concrete. Among all eight statistical parameters that are used in this study, the uncertainty at 95% (U95) is noticed as a more efficient parameter in evaluating the prediction capacity of used models. The proficiency of U_{95} is remarkably noticed to efficiently identify the most efficient predictive modeling approach when other statistical parameters such as coefficient of determination (R^2), mean absolute error (MAE), and Index of Agreement or Willmott (WI) gave almost very close assessments for all comparable models. Furthermore, visualization assessments such as boxplots, scatter plots, and Taylor diagrams have been carried out and pointed out that the SVR-PSO models were the best predictive models in the prediction of CS. Besides, further assessment has been carried out by comparing the performance of the proposed model (SVR-PSO) with 14 models that had been developed in the literature. It is found that the proposed model of this study gave more excellent estimates than the comparable models. Sensitivity analysis using the cosine amplitude method also has been done in this study to select the most influential input parameters on the outputs. It was found that the fine aggregate, coarse aggregate, water, and cement variables have the highest impact on CS, respectively. Finally, the hybridization of SVR with modified PSO provided more accurate CS predictions and thus can help to enhance the understanding of the underlying relations between concrete mix components and CS property.

Using Seven input variables may hinder the performance of the applied models because these variables may have redundant information. Besides, these parameters may be correlated to each other or have uncertainties that reduce the efficiency of the predicted model. For future studies, this study recommends using the PCA approach before training the models to remove the redundant information from input vectors and eliminate the correlation between inputs data.

Abbreviations

AI: Artificial intelligence
ANFIS: Adaptive neuro-fuzzy inference
ANN: Artificial neural networks
CC: Correlation of coefficient
CO_2: Carbon dioxide
CS: Compressive strength
CV: Cross-validation
DT: Decision tree
EFSIMT: Evolutionary fuzzy support vector machine inference model
ELM: Extreme learning machine
ELM-GWO: Extreme learning machine integrated with grey wolf optimizer
erMAX: Maximum absolute percentage relative error
FA: Fly ash
FFNN: Feedforward neural network
FPNN: Fuzzy polynomial neural network
FS: Furnace slag
GA: Genetic algorithm
GGBFS: Ground granulated blast furnace slag
GMDH: Group method of data handling
HPC: High-performance concrete
IQR: Interquartile range
LS-SVR-FA: Least square support vector regression coupled with firefly algorithm
MAE: Mean absolute error
MARE: Mean absolute relative error
MARS: Multivariate adaptive regression spline
MAX: Maximum value
Min: Minimum value
MLR: Multiple linear regression
NE: Nash–Sutcliffe model efficiency coefficient
NEX: Neural-expert system
PSO: Particle swarm algorithm
RE: Relative error
R^2: Correlation of determination
RELM: Regularized extreme learning machine
SC: Soft Computing
SCC: Self-compacting concrete
Std: Standard deviation
SVR: Support vector regression
U_{95}: Uncertainty at 95
WI: Index of Agreement or Willmott
WOA-ANN: Incorporation of the whale optimization algorithm with artificial neural network
XGBoost: Extreme gradient boosting.

Data Availability

The data are available from the corresponding author upon request.

Conflicts of Interest

The authors declare that there are no conflicts of interest.

Acknowledgments

The authors would like to thank Al-Maarif University College for supporting and funding this research.

References

[1] İ. B. Topçu and M. Sarıdemir, "Prediction of compressive strength of concrete containing fly ash using artificial neural networks and fuzzy logic," *Computational Materials Science*, vol. 41, no. 3, pp. 305–311, 2008.

[2] M. Shariati, S. Rafie, Y. Zandi et al., "Experimental investigation on the effect of cementitious materials on fresh and mechanical properties of self-consolidating concrete," *Advances in concrete construction*, vol. 8, no. 3, pp. 225–237, 2019.

[3] P. Chopra, R. K. Sharma, and M. Kumar, "Prediction of compressive strength of concrete using artificial neural network and genetic programming," *Advances in Materials Science and Engineering*, vol. 2016, pp. 1–10, 2016.

[4] M. M. Hameed and M. K. AlOmar, "Prediction of compressive strength of high-performance concrete: hybrid artificial intelligence technique," in *Applied Computing to Support Industry: Innovation and Technology*, pp. 323–335, Springer International Publishing, Cham, 2020.

[5] H. Naderpour, A. H. Rafiean, and P. Fakharian, "Compressive strength prediction of environmentally friendly concrete using artificial neural networks," *Journal of Building Engineering*, vol. 16, pp. 213–219, 2018.

[6] C. Duran Atiş, "Strength properties of high-volume fly ash roller compacted and workable concrete, and influence of curing condition," *Cement and Concrete Research*, vol. 35, no. 6, pp. 1112–1121, 2005.

[7] S. K. Antiohos, V. G. Papadakis, E. Chaniotakis, and S. Tsimas, "Improving the performance of ternary blended cements by mixing different types of fly ashes," *Cement and Concrete Research*, vol. 37, no. 6, pp. 877–885, 2007.

[8] T. Kim, J. M. Davis, M. T. Ley, S. Kang, and P. Amrollahi, "Fly ash particle characterization for predicting concrete compressive strength," *Construction and Building Materials*, vol. 165, pp. 560–571, 2018.

[9] S. Kang, Z. Lloyd, T. Kim, and M. T. Ley, "Predicting the compressive strength of fly ash concrete with the Particle Model," *Cement and Concrete Research*, vol. 137, Article ID 106218, 2020.

[10] M. Shariati, M. S. Mafipour, B. Ghahremani et al., "A novel hybrid extreme learning machine-grey wolf optimizer (ELM-GWO) model to predict compressive strength of concrete with partial replacements for cement," *Engineering with Computers*, vol. 38, no. 1, pp. 757–779, 2020.

[11] G. Li and X. Zhao, "Properties of concrete incorporating fly ash and ground granulated blast-furnace slag," *Cement and Concrete Composites*, vol. 25, no. 3, pp. 293–299, 2003.

[12] L. Lam, Y. L. Wong, and C. S. Poon, "Effect of fly ash and silica fume on compressive and fracture behaviors of concrete," *Cement and Concrete Research*, vol. 28, no. 2, pp. 271–283, 1998.

[13] Y. Poojari and V. Kampilla, "Strength behavior analysis of fiber reinforced fly ash concrete," *Materials Today Proceedings*, vol. 43, pp. 1659–1665, 2021.

[14] D. Suresh and K. Nagaraju, "Ground granulated blast slag (GGBS) in concrete–a review," *IOSR Journal of Mechanical and Civil Engineering*, vol. 12, no. 4, pp. 76–82, 2015.

[15] M. A. Abd-El.Aziz, S. Abd.El.Aleem, and M. Heikal, "Physico-chemical and mechanical characteristics of pozzolanic cement pastes and mortars hydrated at different curing temperatures," *Construction and Building Materials*, vol. 26, no. 1, pp. 310–316, 2012.

[16] E. Özbay, M. Erdemir, and H. İ. Durmuş, "Utilization and efficiency of ground granulated blast furnace slag on concrete properties – a review," *Construction and Building Materials*, vol. 105, pp. 423–434, 2016.

[17] H. Bınıci, M. Y. Durgun, T. Rızaoğlu, and M. Koluçolak, "Investigation of durability properties of concrete pipes incorporating blast furnace slag and ground basaltic pumice as fine aggregates," *Scientia Iranica*, vol. 19, no. 3, pp. 366–372, 2012.

[18] Y. Geng, Z. Wang, L. Shen, and J. Zhao, "Calculating of CO2 emission factors for Chinese cement production based on inorganic carbon and organic carbon," *Journal of Cleaner Production*, vol. 217, pp. 503–509, 2019.

[19] J. Wei and K. Cen, "Empirical assessing cement CO2 emissions based on China's economic and social development during 2001-2030," *The Science of the Total Environment*, vol. 653, pp. 200–211, 2019.

[20] J. An, R. S. Middleton, and Y. Li, "Environmental performance analysis of cement production with CO2 capture and storage technology in a life-cycle perspective," *Sustainability*, vol. 11, no. 9, p. 2626, 2019.

[21] M. Hameed, S. S. Sharqi, Z. M. Yaseen, H. A. Afan, A. Hussain, and A. Elshafie, "Application of artificial intelligence (AI) techniques in water quality index prediction: a case study in tropical region, Malaysia," *Neural Computing & Applications*, vol. 28, no. S1, pp. 893–905, 2017.

[22] Z. Keshavarz and H. Torkian, "Application of ANN and ANFIS models in determining compressive strength of concrete," *Journal of Soft Computing in Civil Engineering*, vol. 2, no. 1, pp. 62–70, 2018.

[23] F. Khademi and K. Behfarnia, "Evaluation OF concrete compressive strength using artificial neural network and multiple linear regression models," *INTERNATIONAL JOURNAL OF OPTIMIZATION IN CIVIL ENGINEERING*, vol. 6, no. 3, 2016, [Online]. Available: https://www.sid.ir/en/journal/ViewPaper.aspx?id=500731.

[24] D. J. Armaghani and P. G. Asteris, "A comparative study of ANN and ANFIS models for the prediction of cement-based mortar materials compressive strength," *Neural Computing & Applications*, vol. 33, no. 9, pp. 4501–4532, 2021.

[25] H.-G. Ni and J.-Z. Wang, "Prediction of compressive strength of concrete by neural networks," *Cement and Concrete Research*, vol. 30, no. 8, pp. 1245–1250, 2000.

[26] J.-J. Lee, D.-K. Kim, S.-K. Chang, and J.-H. Lee, "Application of support vector regression for the prediction of concrete strength," *Computers and Concrete*, vol. 4, no. 4, pp. 299–316, 2007.

[27] K. O. Akande, T. O. Owolabi, T. O. Owolabi, S. Twaha, and S. O. Olatunji, "Performance comparison of SVM and ANN in predicting compressive strength of concrete," *IOSR Journal of Computer Engineering*, vol. 16, no. 5, pp. 88–94, 2014.

[28] H. Ling, C. Qian, W. Kang, C. Liang, and H. Chen, "Combination of Support Vector Machine and K-Fold cross validation to predict compressive strength of concrete in marine environment," *Construction and Building Materials*, vol. 206, pp. 355–363, 2019.

[29] B. K. R. Prasad, H. Eskandari, and B. V. V. Reddy, "Prediction of compressive strength of SCC and HPC with high volume fly ash using ANN," *Construction and Building Materials*, vol. 23, no. 1, pp. 117–128, 2009.

[30] A. M. Abd and S. M. Abd, "Modelling the strength of lightweight foamed concrete using support vector machine (SVM)," *Case Studies in Construction Materials*, vol. 6, pp. 8–15, 2017.

[31] X. Xue, "Evaluation of concrete compressive strength based on an improved PSO-LSSVM model," *Computers and Concrete*, vol. 21, no. 5, pp. 505–511, 2018.

[32] L. Sun, M. Koopialipoor, D. Jahed Armaghani, R. Tarinejad, and M. M. Tahir, "Applying a meta-heuristic algorithm to predict and optimize compressive strength of concrete samples," *Engineering with Computers*, vol. 37, no. 2, pp. 1133–1145, 2021.

[33] D. Zhang, W. Xiang, Q. Cao, and S. Chen, "Application of incremental support vector regression based on optimal training subset and improved particle swarm optimization algorithm in real-time sensor fault diagnosis," *Applied Intelligence*, vol. 51, no. 6, pp. 3323–3338, 2021.

[34] H. Jahangir and D. Rezazadeh Eidgahee, "A new and robust hybrid artificial bee colony algorithm - ANN model for FRP-concrete bond strength evaluation," *Composite Structures*, vol. 257, p. 113160, 2021.

[35] Z. Yuan, L.-N. Wang, and X. Ji, "Prediction of concrete compressive strength: research on hybrid models genetic based algorithms and ANFIS," *Advances in Engineering Software*, vol. 67, pp. 156–163, 2014.

[36] E. Li, J. Zhou, X. Shi et al., "Developing a hybrid model of salp swarm algorithm-based support vector machine to predict the strength of fiber-reinforced cemented paste backfill," *Engineering with Computers*, vol. 37, no. 4, pp. 3519–3540, 2021.

[37] R. Madandoust, J. H. Bungey, and R. Ghavidel, "Prediction of the concrete compressive strength by means of core testing using GMDH-type neural network and ANFIS models," *Computational Materials Science*, vol. 51, no. 1, pp. 261–272, 2012.

[38] M. Shariati, M. S. Mafipour, P. Mehrabi, K. Wakil, N. T. Trung, and A. Toghroli, "Prediction of concrete strength in presence of furnace slag and fly ash using Hybrid ANN-GA (Artificial Neural Network-Genetic Algorithm)," *Smart Structures and Systems*, vol. 25, no. 2, pp. 183–195, 2020.

[39] I.-J. Han, T.-F. Yuan, J.-Y. Lee, Y.-S. Yoon, and J.-H. Kim, "Learned prediction of compressive strength of GGBFS concrete using hybrid artificial neural network models," *Materials*, vol. 12, no. 22, p. 3708, 2019.

[40] F. Özcan, C. D. Atiş, O. Karahan, E. Uncuoğlu, and H. Tanyildizi, "Comparison of artificial neural network and fuzzy logic models for prediction of long-term compressive strength of silica fume concrete," *Advances in Engineering Software*, vol. 40, no. 9, pp. 856–863, 2009.

[41] C. D. Atiş, "High-volume fly ash concrete with high strength and low drying shrinkage," *Journal of Materials in Civil Engineering*, vol. 15, no. 2, pp. 153–156, 2003.

[42] A. Behnood, V. Behnood, M. Modiri Gharehveran, and K. E. Alyamac, "Prediction of the compressive strength of normal and high-performance concretes using M5P model tree algorithm," *Construction and Building Materials*, vol. 142, pp. 199–207, 2017.

[43] I.-C. Yeh, "Modeling slump flow of concrete using second-order regressions and artificial neural networks," *Cement and Concrete Composites*, vol. 29, no. 6, pp. 474–480, 2007.

[44] I.-C. Yeh, "Simulation of concrete slump using neural networks," *Proceedings of the Institution of Civil Engineers - Construction Materials*, vol. 162, no. 1, pp. 11–18, 2009.

[45] H. H. John, "Index," in *Adaptation in Natural and Artificial Systems: An Introductory Analysis with Applications to Biology, Control, and Artificial Intelligence*, pp. 207–211, MIT Press, Cambridge, Massachusetts, United States, 1992.

[46] D. E. Goldenberg, *Genetic Algorithms in Search, Optimization and Machine Learning*, Addison-Wesley, Reading: MA, 1989.

[47] E. Momeni, R. Nazir, D. Jahed Armaghani, and H. Maizir, "Prediction of pile bearing capacity using a hybrid genetic algorithm-based ANN," *Measurement*, vol. 57, pp. 122–131, 2014.

[48] M. Khandelwal and D. J. Armaghani, "Prediction of drillability of rocks with strength properties using a hybrid GA-ANN technique," *Geotechnical & Geological Engineering*, vol. 34, no. 2, pp. 605–620, 2016.

[49] M. Koopialipoor, A. Fallah, D. J. Armaghani, A. Azizi, and E. T. Mohamad, "Three hybrid intelligent models in estimating flyrock distance resulting from blasting," *Engineering with Computers*, vol. 35, no. 1, pp. 243–256, 2019.

[50] M. Beiki, A. Majdi, and A. D. Givshad, "Application of genetic programming to predict the uniaxial compressive strength and elastic modulus of carbonate rocks," *International Journal of Rock Mechanics and Mining Sciences*, vol. 63, pp. 159–169, 2013.

[51] E. T. Mohamad, R. S. Faradonbeh, D. J. Armaghani, M. Monjezi, and M. Z. A. Majid, "An optimized ANN model based on genetic algorithm for predicting ripping production," *Neural Computing & Applications*, vol. 28, no. S1, pp. 393–406, 2017.

[52] J. Kennedy and R. Eberhart, "Particle swarm optimization,"vol. 4, pp. 1942–1948, in *Proceedings of the ICNN'95-International Conference on Neural Networks*, vol. 4, pp. 1942–1948, IEEE, Perth, WA, Australia, 1995.

[53] B. Gordan, D. Jahed Armaghani, M. Hajihassani, and M. Monjezi, "Prediction of seismic slope stability through combination of particle swarm optimization and neural network," *Engineering with Computers*, vol. 32, no. 1, pp. 85–97, 2016.

[54] C. Cortes and V. Vapnik, "Support-vector networks," *Machine Learning*, vol. 20, no. 3, pp. 273–297, 1995.

[55] A. A. Farag and R. M. Mohamed, "Classification of multispectral data using support vector machines approach for density estimation," in *Proceedings of the International conference on intelligent engineering system*, pp. 6–8, Citeseer, 2003.

[56] J. Fan, L. Wu, F. Zhang et al., "Evaluating the effect of air pollution on global and diffuse solar radiation prediction using support vector machine modeling based on sunshine duration and air temperature," *Renewable and Sustainable Energy Reviews*, vol. 94, pp. 732–747, 2018.

[57] X. Ji, X. Shang, R. A. Dahlgren, and M. Zhang, "Prediction of dissolved oxygen concentration in hypoxic river systems using support vector machine: a case study of Wen-Rui Tang River, China," *Environmental Science and Pollution Research*, vol. 24, no. 19, pp. 16062–16076, 2017.

[58] K. Mohammadi, S. Shamshirband, M. H. Anisi, K. A. Alam, and D. Petković, "Support vector regression based prediction of global solar radiation on a horizontal surface," *Energy Conversion and Management*, vol. 91, pp. 433–441, 2015.

[59] K. Roushangar, M. T. Alami, J. Shiri, and M. M. Asl, "Determining discharge coefficient of labyrinth and arced labyrinth weirs using support vector machine," *Hydrology Research*, vol. 49, no. 3, pp. 924–938, 2018.

[60] A. S. Abobakr Yahya, A. N. Ahmed, F. Binti Othman et al., "Water quality prediction model based support vector machine model for Ungauged River catchment under dual scenarios," *Water*, vol. 11, no. 6, p. 1231, 2019.

[61] N. Sapankevych and R. Sankar, "Time series prediction using support vector machines: a survey," *IEEE Computational Intelligence Magazine*, vol. 4, no. 2, pp. 24–38, 2009.

[62] V. Vapnik, *The Nature of Statistical Learning theory*, p. 27, Springer science & business media, Berlin, Germany, 2013.

[63] M. K. AlOmar, M. M. Hameed, N. Al-Ansari, and M. A. AlSaadi, "Data-driven model for the prediction of total dissolved gas: robust artificial intelligence approach," *Advances in Civil Engineering*, vol. 2020, pp. 1–20, 2020.

[64] R. C. Deo, N. Downs, A. V. Parisi, J. F. Adamowski, and J. M. Quilty, "Very short-term reactive forecasting of the solar ultraviolet index using an extreme learning machine integrated with the solar zenith angle," *Environmental Research*, vol. 155, pp. 141–166, 2017.

[65] G.-B. Huang, Q.-Y. Zhu, and C.-K. Siew, "Extreme learning machine: theory and applications," *Neurocomputing*, vol. 70, no. 1-3, pp. 489–501, 2006.

[66] H.-H. Liu, L.-C. Chang, C.-W. Li, and C.-H. Yang, "Particle swarm optimization-based support vector regression for tourist arrivals forecasting," *Computational Intelligence and Neuroscience*, vol. 2018, pp. 1–13, 2018.

[67] I. O. Alade, M. A. Abd Rahman, and T. A. Saleh, "Modeling and prediction of the specific heat capacity of Al2 O3/water nanofluids using hybrid genetic algorithm/support vector regression model," *Nano-Structures & Nano-Objects*, vol. 17, pp. 103–111, 2019.

[68] M. Sornalakshmi, S. Balamurali, M. Venkatesulu et al., "Hybrid method for mining rules based on enhanced Apriori algorithm with sequential minimal optimization in healthcare industry," *Neural Computing & Applications*, 2020.

[69] M. E. H. Pedersen, "Good parameters for particle swarm optimization," Technical Report HL1001, pp. 1551–3203, Hvass Lab, Copenhagen, Denmark, 2010.

[70] E. Mezura-Montes and C. A. Coello Coello, "Constraint-handling in nature-inspired numerical optimization: past, present and future," *Swarm and Evolutionary Computation*, vol. 1, no. 4, pp. 173–194, 2011.

[71] P. G. Asteris, I. Argyropoulos, L. Cavaleri et al., "Masonry compressive strength prediction using artificial neural networks," in *Transdisciplinary Multispectral Modeling and Cooperation for the Preservation of Cultural Heritage*, pp. 200–224, Springer International Publishing, Cham, 2019.

[72] M. K. AlOmar, M. M. Hameed, and M. A. AlSaadi, "Multi hours ahead prediction of surface ozone gas concentration: robust artificial intelligence approach," *Atmospheric Pollution Research*, vol. 11, no. 9, pp. 1572–1587, 2020.

[73] H. Tao, A. A. Ewees, A. O. Al-Sulttani et al., "Global solar radiation prediction over North Dakota using air temperature: development of novel hybrid intelligence model," *Energy Reports*, vol. 7, pp. 136–157, 2021.

[74] G. Zhang, Z. H. Ali, M. S. Aldlemy et al., "Reinforced concrete deep beam shear strength capacity modelling using an integrative bio-inspired algorithm with an artificial intelligence model," *Engineering with Computers*, 2020.

[75] J.-S. Chou, C.-K. Chiu, M. Farfoura, and I. Al-Taharwa, "Optimizing the prediction accuracy of concrete compressive strength based on a comparison of data-mining techniques," *Journal of Computing in Civil Engineering*, vol. 25, no. 3, pp. 242–253, 2011.

[76] A.-D. Pham, N.-D. Hoang, and Q.-T. Nguyen, "Predicting compressive strength of high-performance concrete using metaheuristic-optimized least squares support vector regression," *Journal of Computing in Civil Engineering*, vol. 30, no. 3, p. 06015002, 2016.

[77] D. T. Bui, M. a. M. Abdullahi, S. Ghareh, H. Moayedi, and H. Nguyen, "Fine-tuning of neural computing using whale optimization algorithm for predicting compressive strength of concrete," *Engineering with Computers*, vol. 37, no. 1, pp. 701–712, 2019.

[78] M. R. Kaloop, D. Kumar, P. Samui, J. W. Hu, and D. Kim, "Compressive strength prediction of high-performance concrete using gradient tree boosting machine," *Construction and Building Materials*, vol. 264, p. 120198, 2020.

[79] I.-C. Yeh, "Modeling of strength of high-performance concrete using artificial neural networks," *Cement and Concrete Research*, vol. 28, no. 12, pp. 1797–1808, 1998.

[80] R. Gupta, M. A. Kewalramani, and A. Goel, "Prediction of concrete strength using neural-expert system," *Journal of Materials in Civil Engineering*, vol. 18, no. 3, pp. 462–466, 2006.

[81] M. H. Fazel Zarandi, I. B. Türksen, J. Sobhani, and A. A. Ramezanianpour, "Fuzzy polynomial neural networks for approximation of the compressive strength of concrete," *Applied Soft Computing*, vol. 8, no. 1, pp. 488–498, 2008.

[82] I.-C. Yeh and L.-C. Lien, "Knowledge discovery of concrete material using Genetic Operation Trees," *Expert Systems with Applications*, vol. 36, no. 3, pp. 5807–5812, 2009.

[83] M.-Y. Cheng, J.-S. Chou, A. F. V. Roy, and Y.-W. Wu, "High-performance concrete compressive strength prediction using time-weighted evolutionary fuzzy support vector machines inference model," *Automation in Construction*, vol. 28, pp. 106–115, 2012.

[84] A. K. Al-Shamiri, T.-F. Yuan, and J. H. Kim, "Non-tuned machine learning approach for predicting the compressive strength of high-performance concrete," *Materials*, vol. 13, no. 5, p. 1023, 2020.

[85] Z. Wan, Y. Xu, and B. Šavija, "On the use of machine learning models for prediction of compressive strength of concrete: influence of dimensionality reduction on the model performance," *Materials*, vol. 14, no. 4, p. 713, 2021.

[86] M. M. Hameed, M. K. AlOmar, W. J. Baniya, and M. A. AlSaadi, "Prediction of high-strength concrete: high-order response surface methodology modeling approach," *Engineering with Computers*, 2021.

[87] X. Ji and S. Y. Liang, "Model-based sensitivity analysis of machining-induced residual stress under minimum quantity lubrication," *Proceedings of the Institution of Mechanical Engineers - Part B: Journal of Engineering Manufacture*, vol. 231, no. 9, pp. 1528–1541, 2017.